AIP Advances

Image-based feedback control of a magnetic catheter to enhance the path-following capability of the position and orientation at its distal part

Cite as: AIP Advances **9**, 125127 (2019); https://doi.org/10.1063/1.5129309
Submitted: 29 September 2019 • Accepted: 15 November 2019 • Published Online: 20 December 2019

N. Kim, W. Lee, E. Jung, et al.

Image-based feedback control of a magnetic catheter to enhance the path-following capability of the position and orientation at its distal part

Cite as: AIP Advances 9, 125127 (2019); doi: 10.1063/1.5129309
Presented: 6 November 2019 • Submitted: 29 September 2019 •
Accepted: 15 November 2019 • Published Online: 20 December 2019

N. Kim, W. Lee, E. Jung, J. Kim, J. Park, and G. Jang[a)]

AFFILIATIONS

PREM, Department of Mechanical Engineering, Hanyang University, Seoul 04763, Korea

Note: This paper was presented at the 64th Annual Conference on Magnetism and Magnetic Materials.
[a)]Gunhee Jang is a corresponding author. **Electronic mail:** ghjang@hanyang.ac.kr

ABSTRACT

We have proposed a novel image-based feedback control method to enhance the path-following capability for position and orientation of a magnetic catheter at its distal part. The proposed control method uses only a navigation status of the magnetic catheter for manipulation without utilizing complex analytical models. By comparing the positions of two markers of the magnetic catheter relative to a predefined path, we classify the navigation status of the magnetic catheter into four cases and determine the external magnetic field and feeding velocity according to a proposed control algorithm. Finally, we conduct a path-following experiment in an environment with multiple branches to verify the improved position and minimization of the orientation error regarding the path-following capability of the proposed control method.

I. INTRODUCTION

A catheter is a long flexible tube inserted into the body to deliver drugs or treatment devices to a target lesion. Conventional catheters are manipulated by the hands of a medical doctor from outside the patient's body, exhibiting low steering capability and maneuverability. To overcome these limitations, magnetic catheters (MCs), which have permanent magnets at the distal part, are widely investigated nowadays.[1] Magnetic torque is generated at the embedded magnets when an external magnetic field (EMF) is applied, and the MC can be actively manipulated using the magnetic torque for better steering capability and maneuverability.

Various analytical models have been utilized to estimate the motions of the MC such as Euler-Bernoulli beam theory[2,3] or Cosserat rod theory.[4] However, control methods based on complex analytical models have several limitations to their application in real *in-vivo* operations. First, they cannot consider the full set of dynamic real-time boundary conditions such as friction and reaction forces. Moreover, since complex analytical models require computation time for numerical calculations, the control method makes MC manipulation challenging in real-time due to time-delay. Additionally, most of the conventional control methods control the position of only one distal point of the MC. However, in the case of the MC equipped with treatment modules at its distal part, the orientation of the MC should be controlled as well to prevent damage which may be caused by contact between the treatment modules and the inner wall of the environment.

We propose a novel image-based feedback control (IBFC) method of the MC utilizing the positions of two markers located at both ends of the distal part without analytical models. In the IBFC method, the normal pixel distances between each marker and a predefined path are calculated, and the status of the MC is classified into one of four cases depending on the normal pixel distances. For each case, we set different values for the feeding velocity of the MC and angular velocity of the EMF to minimize both the position and orientation error. The proposed IBFC method was verified by controlling a MC in an environment with multiple branches. Further, to validate the path-following performance of the proposed IBFC method, trajectories and average position error of each marker were measured and compared with the results obtained

by controlling the MC using the conventional one-point control method.

II. MANIPULATION OF THE MC USING THE IBFC METHOD

Figure 1 shows the structure of the MC and an overall procedure of the proposed IBFC method. The MC has three permanent magnets to generate magnetic torque under an EMF and two markers at both ends of the distal part for tracking. The magnetic torque generated at the magnets under the EMF can be expressed as follows:[3]

$$\mathbf{T} = \mathbf{m} \times \mathbf{B} \tag{1}$$

where **m** and **B** are the magnetic moment of the magnets and the magnetic flux density of the EMF, respectively. Since the magnetic torque aligns the magnets with the direction of the EMF, a magnetic navigation system (MNS) that generates and control the EMF can manipulate the direction of the MC. A feeding device pushes and pulls the MC axially. A path composed of several line segments is predefined by the operator, and navigation status is determined by comparing the normal distances between each marker and the nearest line segment. Based on the current status of the MC, the IBFC method controls angular velocity of the EMF (ω_{EMF}) and feeding velocity of the MC (v_F) by utilizing the MNS and the feeding device, respectively, to maximize the path-following capability.

First, a camera captures real-time images of the workspace, and the RGB color tracking module detects the markers from the images. The positions of the markers are transferred to the status classification module, which calculates the normal distance between the markers and n^{th} line segment to identify the navigation status of the MC. The normal distance (d_q) between marker q and n^{th} line segment shown in Figure 2(a) can be calculated as follows:

$$d_q = \frac{(y_{n+1} - y_n)(x_q - x_n) - (x_{n+1} - x_n)(y_q - y_n)}{\sqrt{(y_{n+1} - y_n)^2 + (x_{n+1} - x_n)^2}}, \quad \begin{cases} q = 1 \text{ for a front marker} \\ q = 2 \text{ for a rear marker} \end{cases} \tag{2}$$

where (x_n, y_n), (x_{n+1}, y_{n+1}), and (x_q, y_q) are the pixel positions of n^{th} and $(n+1)^{\text{th}}$ points composing the n^{th} line segment and the pixel position of marker q, respectively. From the image acquisition of the workspace to the calculation of the normal distance, all procedures progress based on the pixel coordinates without any calibration process for mapping to real coordinates. This minimizes the errors of the control system, which may be caused by the distortion of the lens and imprecise calibration.

Then, the navigation status of the MC is classified into one of four cases, as shown in Figure 2(b), by the status classification module. When both markers are close enough to the predefined path that both d_1 and d_2 are smaller than d_{allow} (which is set by the operator), this status is categorized to case A. In case A, v_F and ω_{EMF} are maximized and minimized, respectively, for fast and effective navigation. If any marker has normal distance greater than d_{allow}, the status is categorized depending on the signs of d_1 and d_2. When d_1 and d_2 have same sign, the status is categorized as case B, and v_F and ω_{EMF} are minimized and maximized, respectively, to approach the path quickly. If d_1 and d_2 have different sign, the status is categorized as case C or D depending on which is smaller. For cases C and D, v_F and ω_{EMF} are selected differently to minimize d_1 and d_2 simultaneously. The determined v_F and ω_{EMF} are transmitted to the feeding device and the MNS to manipulate the MC. This categorization process is

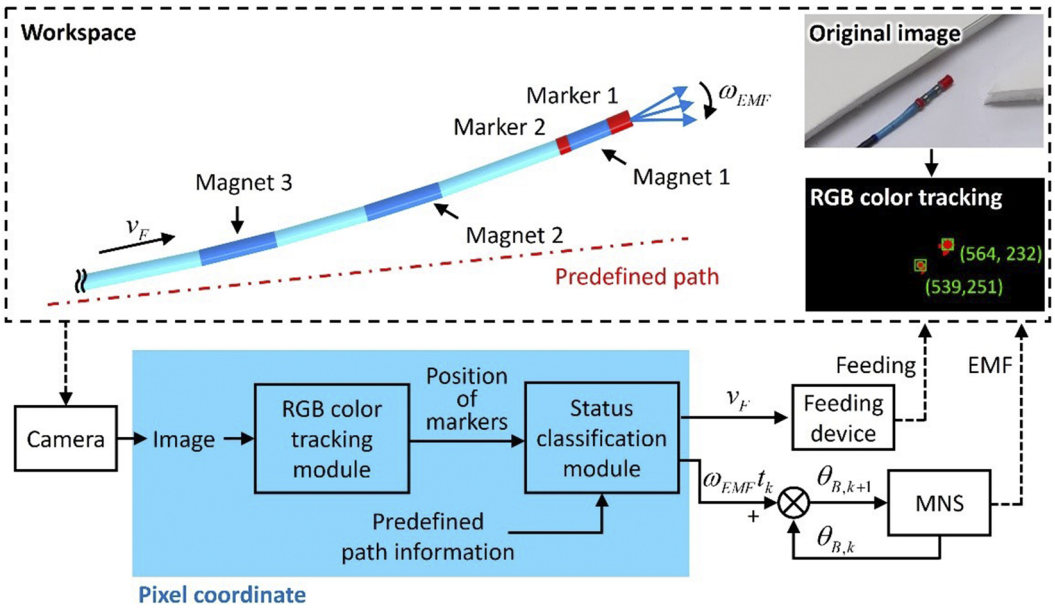

FIG. 1. Structure of the MC and an overall procedure of the proposed IBFC method.

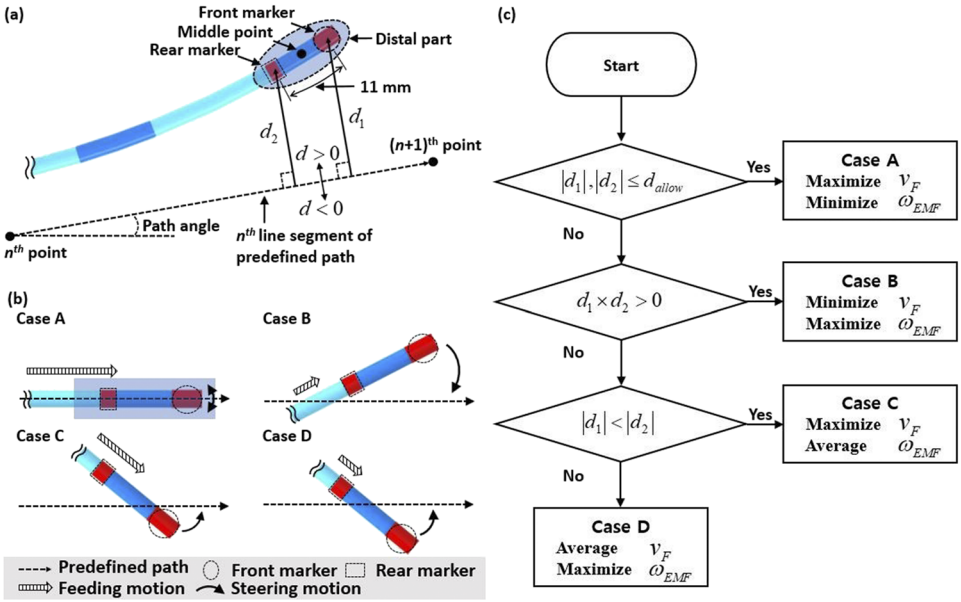

FIG. 2. (a) Normal distances between two markers and the predefined path composed of several line segments. (b) Four cases of navigation status of the MC. (c) Flow chart to classify the status of the MC into one of the four cases and determine suitable values for v_F and ω_{EMF}.

represented in Figure 2(c) as a flow chart. Assuming the current iteration is the k^{th}, the direction of the EMF for the next iteration (θ_{k+1}) is calculated as follows:

$$\theta_{k+1} = \theta_k + \omega_{EMF} t_k \tag{3}$$

where θ_k and t_k are the direction of the EMF and a measured processing time for the k^{th} iteration of the IBFC method, respectively.

III. RESULTS AND DISCUSSION

To manipulate the MC, the feeding device and closed-loop magnetic navigation system (CMNS) were utilized, as shown in Figures 3(a) and (b). The feeding device consists of three step motors (*17HD2041-04N-A*, MOONS motor, China) and generates translational and rotational motion of the MC. The CMNS composed of eight electromagnets and backyoke structure can generate EMF in all three-dimensional directions in the workspace.[6] A commercial MC (*Thermocool*®, Biosense Webster, USA) with two visual markers shown in Figure 3(c) was used to verify the IBFC.

The proposed IBFC method was verified by controlling the MC in an environment with multiple branches. We first predefined the path to a target branch, then manipulated the MC using the IBFC method. To verify the effectiveness of the IBFC method based on the two markers, we conducted an experiment using a control method based on a single marker at the distal tip of the MC. The control method based on a single marker is similar to the IBFC method but manipulates the MC just to minimize the position error of front marker without status classification. The rear marker is not utilized to control the MC in the control method based on a single marker, but it is used to evaluate the path following capability of the whole distal part of MC. v_F and ω_{EMF} were set to the average values of the minimum and maximum values for the IBFC method. During manipulation, the positions of the markers were tracked in real-time

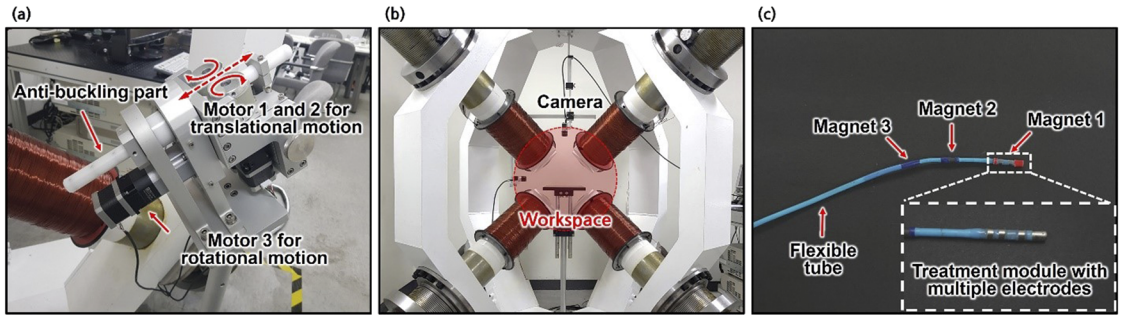

FIG. 3. (a) Feeding device, (b) closed-loop magnetic navigation system (CMNS) and (c) commercial MC used for the experiment.

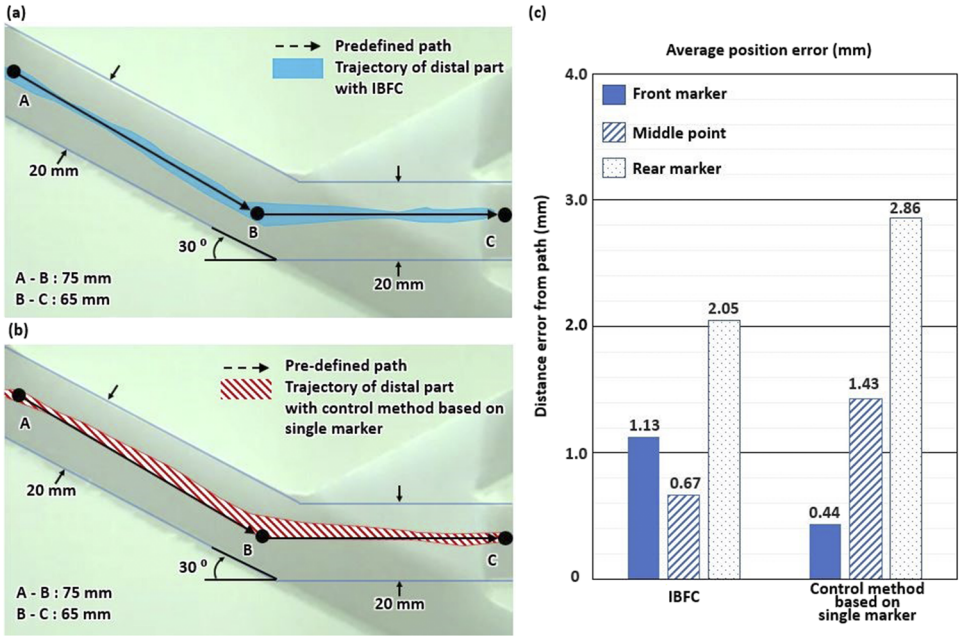

FIG. 4. Trajectories in which the distal part of the MC sweep during navigation with (a) the proposed IBFC and (b) the control method based on a single marker. (c) Average normal distance errors of two markers and a middle point between the front and rear markers.

by an RGB camera (acA2000-165uc, BASLER, Germany) and by utilizing color tracking algorithms. We set d_{allow}, the maximum and minimum v_F, and the maximum and minimum ω_{EMF} to be 12 pixels (≈2 mm), 1.2 mm/s, 0.3 mm/s, $\frac{\pi}{60}$ rad/s, and $\frac{\pi}{180}$ rad/s, respectively. The magnitude of the EMF at the center of the workspace was fixed to 40 mT.

According to results represented in Figures 4(a) and (b), the MC manipulated by the IBFC method tends to maintain its distal part near the center of the predefined path without biasing towards the inner wall closer than the MC manipulated by the control method based on a single marker. To evaluate how good the whole distal part of the MC follows the path for each control method, we consider the normal distances of the front marker, the rear marker and the middle point of the front and rear markers comprehensively. Figure 4(c) shows the average normal distance errors of two markers and a middle point between the front and rear markers. The results show that the proposed IBFC method has better position accuracy at the middle point and the rear marker than the control method based on a single marker. Also, the total position error and the orientation error of each iteration during the navigation represented in Figures 4(a) and (b) were calculated as follows:

$$|d_{1,n}| + \left|\frac{d_{1,n} + d_{2,n}}{2}\right| + |d_{2,n}| = e_{position,n} \tag{4}$$

$$|d_{1,n} - d_{2,n}| = e_{orientation,n} \tag{5}$$

where $d_{1,n}$, $d_{2,n}$, $e_{position,n}$ and $e_{orientation,n}$ are the normal distances of the front and rear markers, and the total position and orientation errors of the n^{th} iteration, respectively. The average position error and the average orientation error of the IBFC method were calculated from the total position error and orientation error from 1^{st} to n^{th} iterations and reduced by 18.64% and 7.5% compared to them of the control method based on a single marker, respectively. The average processing time for one iteration of the IBFC method (t_k) was 0.1 second, which is sufficient for real-time control of the MC. Therefore, the proposed IBFC method has not only good path-following capability without the use of complex analytical models, but also short processing time, which is necessary for real-time control of medical operations.

IV. CONCLUSION

We developed IBFC method for the MC to enhance the path-following capability of the position and orientation at its distal part. The proposed IBFC method calculates the normal distances of each marker, classifies the status of MC into one of four cases, and determines v_F and ω_{EMF} to minimize d_1 and d_2 simultaneously for each case. We verified the proposed IBFC method by controlling the MC. According to the results, the IBFC method showed good accuracy regarding the position and orientation related to the path-following capability and fast processing for real-time control of the MC. This research contributes to improving the accuracy and safety of MC manipulation and to expanding the biomedical applications of MC and magnetic manipulation methods.

ACKNOWLEDGMENTS

This research was supported by a grant of the Korea Health Technology R&D Project through the Korea Health Industry Development Institute (KHIDI), funded by the Ministry of Health & Welfare, Republic of Korea (grant number: HI19C0642)

REFERENCES

[1]H. Christoff, S. Jakub, and M. Sarthak, "Flexible instruments for endovascular interventions: Improved magnetic steering, actuation, and image-guided surgical instruments," IEEE Robotics and Automation Magazine **25**, 71–82 (2018).
[2]Vi N. T. Le, N. H. Nguyen, and P. Pratten, "Accurate modeling and positioning of a magnetically controlled catheter tip: Accurate modeling and positioning of a magnetically controlled catheter tip," Medical Physics **43**, 650–663 (2016).
[3]N. Kim, S. Lee, and G. Jang, "Development of a magnetic catheter with rotating multi-magnets to achieve unclogging motions with enhanced steering capability," AIP Advances **8**, 056708 (2018).
[4]J. Edelmann, A. J. Petruska, and B. J. Nelson, "Magnetic control of continuum devices," The International Journal of Robotics Research **36**, 68–85 (2017).
[5]S. Jeon and G. Jang, "Precise steering and unclogging motions of a catheter with a rotary magnetic drill tip actuated by a magnetic navigation system," IEEE Transactions on Magnetics **48**, 4062–4065 (2012).
[6]J. Nam, W. Lee, E. Jung, and G. Jang, "Magnetic navigation system utilizing a closed magnetic circuit to maximize magnetic field and a mapping method to precisely control magnetic field in real time," IEEE Transactions on Industrial Electronics **65**, 5673–5681 (2018).